AGU PUBLICATIONS

Journal of Advances in Modeling Earth Systems

RESEARCH ARTICLE

10.1002/2016MS000631

Recirculation and growth of raindrops in simulated shallow cumulus

A. K. Naumann[1] and A. Seifert[2]

[1]Max Planck Institute for Meteorology, Hamburg, Germany, [2]Hans-Ertel Centre for Weather Research, Deutscher Wetterdienst, Hamburg, Germany

Key Points:
- Raindrop growth in a field of shallow cumuli is simulated with a Lagrangian drop model
- Recirculating raindrops contribute up to 50% to the surface precipitation per cloud
- Accretion and selfcollection-dominated growth regimes are identified for simulated raindrops

Correspondence to:
A. K. Naumann,
ann-kristin.naumann@mpimet.mpg.de

Citation:
Naumann, A. K., and A. Seifert (2016), Recirculation and growth of raindrops in simulated shallow cumulus, *J. Adv. Model. Earth Syst.*, *08*, doi:10.1002/2016MS000631.

Received 12 JAN 2016
Accepted 23 MAR 2016
Accepted article online 25 MAR 2016

Abstract This study investigates growth processes of raindrops and the role of recirculation of raindrops for the formation of precipitation in shallow cumulus. Two related cases of fields of lightly precipitating shallow cumulus are simulated using Large-Eddy Simulation combined with a Lagrangian drop model for raindrop growth and a cloud tracking algorithm. Statistics from the Lagrangian drop model yield that most raindrops leave the cloud laterally and then evaporate in the subsaturated cloud environmental air. Only 1%–3% of the raindrops contribute to surface precipitation. Among this subsample of raindrops that contribute to surface precipitation, two growth regimes are identified: those raindrops that are dominated by accretional growth from cloud water, and those raindrops that are dominated by selfcollection among raindrops. The mean cloud properties alone are not decisive for the growth of an individual raindrop but the in-cloud variability is crucial. Recirculation of raindrops is found to be common in shallow cumulus, especially for those raindrops that contribute to surface precipitation. The fraction of surface precipitation that is attributed to recirculating raindrops differs from cloud to cloud but can be larger than 50%. This implies that simple conceptual models of raindrop growth that neglect the effect of recirculation disregard a substantial portion of raindrop growth in shallow cumulus.

1. Introduction

Despite the small amount of precipitation produced by shallow cumulus, its precipitation and especially the evaporation of precipitation are known to influence the boundary layer structure, e.g., by the formation of cold pools, which are important for the organization of shallow cumulus [*Jensen et al.*, 2000; *Seifert and Heus*, 2013]. To represent those effects adequately, an appropriate representation of rain microphysical processes is essential. Bulk microphysics parameterization, especially when applied to models with coarse resolution, are known to encounter biases if they do not account for subgrid-scale variability [*Pincus and Klein*, 2000; *Chosson et al.*, 2014]. In addition to the subgrid-scale variability of the bulk fields, the microphysical process rates also depend on the raindrop size distribution (RSD) and therefore on the growth history of individual raindrops. Depending on the complexity of the raindrops' growth histories, the development of the RSD is difficult to parameterize from local variables (in space and time). In this study, we aim to investigate the growth history of raindrops after the initial cloud droplet phase, and the role of recirculation for the formation of precipitation.

In the last decades, most microphysical process studies for warm rain formation have focused on the broadening of the cloud droplet size distribution and on the condensation-coalescence bottleneck of cloud droplet growth, the so-called size gap, which describes the (lack of) growth of cloud droplets in a size range of 10–30 μm in radius, where neither condensation nor collision-coalescence is thought to be very effective [*Simpson*, 1941; *Langmuir*, 1948]. There is emerging agreement that small-scale turbulence does not enhance condensational growth of cloud droplets significantly but that the onset of precipitation is accelerated through small-scale turbulence by enhancing collision rates of cloud droplets (for reviews on this topic see, e.g., *Vaillancourt and Yau* [2000], *Shaw* [2003], and *Grabowski and Wang* [2013]). Small-scale turbulence is also essential for large-eddy hopping, i.e., it allows cloud droplets to move from one large eddy to another. Due to large-eddy hopping, cloud droplets originally located in the vicinity of a single point experience different condensational growth histories, which broadens the observed droplet size distribution [*Cooper*, 1989; *Lasher-Trapp et al.*, 2005; *Bewley and Lasher-Trapp*, 2011; *Devenish et al.*, 2012; *Grabowski and Wang*, 2013].

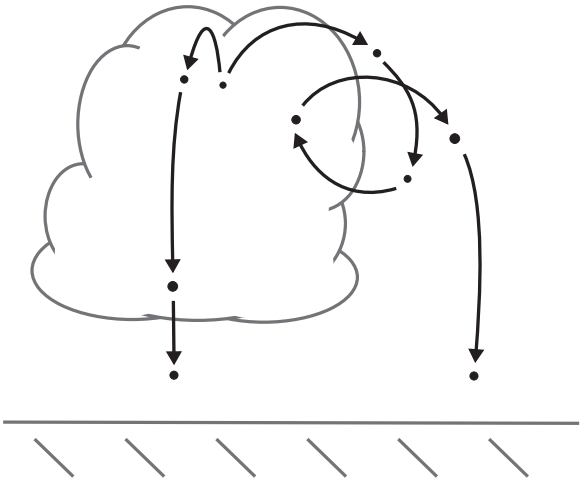

Figure 1. Possible trajectories of raindrops in a shallow cumulus cloud. Raindrops typically emerge near cloud top but their subsequent growth history is less well known. Do raindrops fall straight through the cloud toward the surface or do some of them recirculate in the cloud layer?

As opposed to cloud droplet growth, raindrop growth beyond the size gap has attracted far less attention, and the role of small-scale turbulence and large-eddy hopping for the growth history of drizzle drops and raindrops is less clear. For stratocumulus, the in-cloud residence time of raindrops is found to be decisive for whether raindrops reach the subcloud layer and subsequently also the surface [*Stevens et al*., 1996; *Feingold et al*., 1996; *Kogan*, 2006]. Using Lagrangian parcels, *Pinsky et al*. [2008] and *Magaritz et al*. [2009] argue that a certain fraction of parcels, which exceed a threshold in liquid water content, is needed to trigger drizzle and that mixing plays an important role in this process [*Magaritz-Ronen et al*., 2014, 2016]. Using an idealized single cloud setup, *Cooper et al*. [2013] find that also for cumulus, raindrop embryos need favorable cloud water conditions to significantly contribute to precipitation. To trigger precipitation, only a small fraction of raindrops has to be statistically fortunate enough to experience such beneficial conditions [*Telford*, 1955; *Kostinski and Shaw*, 2005].

To investigate the growth history of raindrops and the role of recirculation in this process, a Lagrangian particle framework has clear advantages over a Eulerian approach because particle trajectory information is generated and can be analyzed. Lagrangian approaches of different complexity have been used, e.g., in combination with direct numerical simulation to study the growth of cloud droplets near the stratocumulus top (A. de Lozar and L. Müßle, Long-resident droplets at the stratocumulus top, submitted to *Journal Atmospheric Chemistry and Physics*, 2016) or to analyze the role of recirculation in the context of ice particle growth and hail formation [e.g., *Browning*, 1964; *Browning and Foote*, 1976; *Knight*, 1990]. In a recent study, *Yang et al*. [2015] use Lagrangian ice particle tracking to show that ice particles in mixed-phase stratiform clouds can be trapped in large-eddy structures, recirculate, and hence experience long lifetimes.

In this paper, we study the growth history of raindrops in a field of shallow cumulus clouds using a Lagrangian drop (LD) model. In particular, we ask two questions: which microphysical processes are important in the growth history of raindrops that finally reach the ground? And: what is the role of recirculation of raindrops for the formation of precipitation (Figure 1)? To investigate these questions, we combine Eulerian Large-Eddy Simulation (LES) of a field of shallow cumulus with the LD model for raindrop growth described by *Naumann and Seifert* [2015]. By additionally applying a cloud tracking algorithm on the LES fields, the LD's trajectories are also analyzed in the context of the temporal development of the cloud entity they originate from.

The rest of this paper is structured as follows: in section 2, we describe the model setup. In section 3, we characterize the behavior of raindrops in a field of shallow cumulus analyzing cloud field statistics and LD statistics. Then in section 4, we discuss the growth mechanisms of raindrops focusing first on accretion and selfcollection, and then on the role of recirculation. Finally, in section 5, we conclude our results.

2. Model Setup

2.1. Large-Eddy Simulation

We use the University of California, Los Angeles LES (UCLA-LES) [*Stevens et al*., 2005; *Stevens*, 2007] with a third-order Runge-Kutta time stepping scheme. Prognostic equations are solved for the three components of the velocity, the total water mixing ratio, the liquid water potential temperature, the mass mixing ratio of rainwater, and the mass-specific number of raindrops. Warm cloud and rain microphysical processes are parameterized by the two-moment bulk microphysics scheme of *Seifert and Beheng* [2001] with a diagnostic

shape parameter [*Seifert*, 2008] and a fixed cloud droplet number density. We adjusted the density correction exponent in the terminal fall velocity to 0.35 to better fit the behavior of small raindrops. Subgrid-scale fluxes are modeled with the Smagorinsky-Lilly model.

2.2. Lagrangian Drop Model

The LD model simulates raindrop growth on a particle-based level after the initial formation of drizzle drops. Details of the LD model and its sensitivity to different model parameters can be found in *Naumann and Seifert* [2015]. The methodology is closely related to the superdroplet method [*Shima et al*., 2009; *Andrejczuk et al*., 2010; *Riechelmann et al*., 2012], but focuses solely on the raindrop phase. Each LD represents a *multiplicity* of real raindrops with the same properties, i.e., the same grid box coordinates, size, and velocity. The LD model does not replace the bulk rain microphysics scheme, instead it is one-way coupled with the Eulerian LES fields.

The LDs are initialized proportional to the autoconversion rate of the bulk microphysics scheme [*Naumann and Seifert*, 2015, section 3.1 therein]. All relevant microphysical processes are included so that the mass of an LD evolves according to the environmental fields of the Eulerian LES: LDs grow due to accretion of bulk cloud water (equation (7) therein) and due to selfcollection among the LDs (equations (8)–(13) therein). LDs evaporate and therefore shrink in undersaturated air (equation (6) therein). The momentum equation for each LD includes dynamical effects such as sedimentation and inertia, and a contribution from the parameterized subgrid-scale fluid velocity (equations (1) and (2) therein). *Naumann and Seifert* [2015] show that the uncertainty of the LD model is much smaller than the uncertainty caused by the choice of the shape parameter in a two-moment bulk rain microphysics scheme.

To analyze the LDs' trajectories and their growth histories, all LDs have a unique identification number and their properties are saved to output files every 15 s. The process of selfcollection, i.e., the collision-coalescence of pairs of LDs, introduces some ambiguity in the history of individual LDs. After each selfcollection event, one of the two LDs that coalesce decreases in multiplicity but retains its mass [*Naumann and Seifert*, 2015, equations (8)–(11) therein]. Obviously, this LD keeps its trajectory and its growth history also after the selfcollection event. The second LD retains its multiplicity but gains mass from the first LD, i.e., after the selfcollection event, this growing LD consists of its original mass plus the mass of the first LD. Therefore, it is not per se clear what the history of this growing LD is. In the LD model, we choose to keep the history of the growing LD in analog to keeping the history of the first LD. Because usually the original mass of the growing LD is larger than the contribution from the first LD, this means that usually the history of an LD is chosen such that it represents the larger fraction of its mass. However, the opposite case may occur too.

In general, other ways to attribute an LD's history after a selfcollection event are possible. For instance, one may attribute the history of that LD that contributes the larger fraction of the new mass to the growing LD. This would imply that sometimes after the selfcollection event the original history of the growing LD is discarded and that both LDs then have the same history. Another possibility might be to calculate an average history of the two original LDs, possibly weighted by their contribution to the growing mass. However, it is not clear what kind of an average history would be meaningful.

2.3. Cloud Tracking

To be able to attribute an LD to a particular cloud and to analyze the temporal development of individual clouds, the cloud tracking of *Heus and Seifert* [2013] is applied to the LES fields. The algorithm tracks cloudy areas in (horizontal) space and time using a cloud liquid water path threshold of 5 g/m^2. A cloud splitting algorithm is necessary to distinguish cloudy objects that are connected in cloud liquid water path at a given time, but that have individual cores and largely keep their own properties. For the splitting, cores are defined as columns where the maximum in-cloud virtual potential temperature excess is larger than 0.5 K, and a region growing algorithm is used to allocate a cloudy area to a core. In this study, cloudy areas that have a cloud core are called *active clouds*. An active cloud can be both a single core cloud or a part of a multicore cloud system. Cloudy regions that have no cloud core are called passive clouds or remnants as in *Heus and Seifert* [2013].

Table 1. Characteristic Properties of the Cloud Field for the Standard RICO Simulation and the Moist RICO Simulation[a]

	C (%)	LWP (g/m^2)	h_{base} (m)	w_{max} (m/s)	RWP_{LD} (g/m^2)	R_{bulk} (mm/d)	R_{LD} (mm/d)
standard RICO	15	11.3	600	7.4	0.8	0.0002	0.0006
moist RICO	20	19.6	600	7.5	4.0	0.0029	0.0032

[a]C, cloud cover; LWP, cloud liquid water path; h_{base}, cloud base height; w_{max}, maximum vertical velocity; RWP_{LD}, rainwater path from the LD model; R_{bulk}, surface precipitation rate from bulk microphysics; R_{LD}, surface precipitation rate from LD model. All values are averaged over 4 h simulation time.

2.4. Case Setup

We use two variants of a case study of shallow cumulus over the ocean (Rain in shallow cumulus over the ocean, RICO) [see *Rauber et al*., 2007]. The initial data and the large-scale forcing for the standard RICO simulations are described by *van Zanten et al*. [2011]. A modified moister version, which differs from the standard setup only by a moister initial profile, is described by *Stevens and Seifert* [2008]. The moister simulation produces more surface precipitation and, as will be shown in section 4.1, LD growth by selfcollection plays a more pronounced role than for the standard RICO simulation.

To simulate a field of shallow cumulus clouds with a sufficient sample of individual clouds, we use a domain size of 12.8^2 km^2. Such a field of shallow cumulus clouds allows us to investigate possible interactions between individual clouds and gives robust statistics in terms of the variability of individual clouds. For both the standard and the moist RICO simulation, the domain height is 3.2 km and the grid spacing is 25 m in all three spatial directions. The time step is 1 s. After a spin-up time of 7 h for the Eulerian LES, both simulations are run for 4 h including the LD model.

We choose an initial multiplicity of 5×10^8, i.e., at initialization, each LD represents 5×10^8 real raindrops. Over the course of the simulations, this in total results in 3.9×10^6 LDs for the standard RICO simulation and 10.1×10^6 LDs for the moist RICO simulation. Note that although the number of LDs is fairly large, the multiplicity is also large, i.e., we sample only a very small fraction of the real raindrops. For individual shallow cumulus, *Naumann and Seifert* [2015, p. 1139 therein] show that statistical properties such as the surface precipitation rate or the slope of the RSD are not sensitive to changes in the initial multiplicitiy in the order of magnitude used here.

3. Characterization of Raindrops in a Field of Shallow Cumulus

3.1. Cloud Field Statistics

In terms of cloud field properties, the moist RICO simulation is characterized by a higher cloud cover, a higher cloud liquid water path, and a higher rainwater path than the standard RICO simulation (Table 1). Consequently, also the surface precipitation rate is higher for the moist RICO simulation than for the standard RICO simulation although the absolute values are low for both simulations.

For both simulations, the results of the bulk rain microphysics scheme compare relatively well with the LD model and the largest differences are found for the surface precipitation rate. For the moist RICO simulation, the surface precipitation rate is slightly lower for the bulk rain microphysics scheme than for the LD model (0.0003 mm/d, Table 1). Although the total surface precipitation rate is lower for the standard RICO simulation, the difference between the bulk rain microphysics scheme and the LD model is larger (0.0004 mm/d). For both simulations, the onset of surface precipitation events is abrupter in the LD model than in the bulk rain microphysics scheme (not shown). This abrupter onset is attributed to a broader RSD for the LDs in the mature state of the cloud's lifecycle, i.e., to more numerous large raindrops that have a high fall speeds and therefore reach the surface earlier. A detailed comparison of the bulk rain microphysics scheme with the LD model for the same case setup but on a smaller domain is given in *Naumann and Seifert* [2016]. In the following, we will discuss rainwater properties only as they are simulated with the LD model. Cloud water properties including the autoconversion rate are not simulated with the LD model and will therefore be discussed as they are simulated with the Eulerian model, i.e., the bulk microphysics scheme. Cloud field statistics are obtained from the cloud tracking.

For the standard RICO simulation, 520 active clouds are tracked in the course of the 4 h simulation excluding those clouds that already exist at the beginning of the simulation and those that still exist at the end of

the simulation. Of those 520 clouds only 10 clouds produce surface precipitation. For the moist RICO simulation, there are overall fewer active clouds (308) of which more (23) produce surface precipitation. In particular, the small clouds are more numerous in the standard RICO simulation while there are slightly more of the largest clouds in the moist RICO simulation. For both simulations, only the largest clouds, which are also the ones that live longest and where most of the LDs originate from, produce surface precipitation (Figures 2a–2c). The average lifetime of an active cloud is 16 min for the standard RICO simulation and 15 min for the moist RICO simulation. Those short-lived clouds do not have enough time for a significant broadening of the cloud droplet size distribution. Therefore, their autoconversion rate remains low and no surface precipitation is produced. In contrast, the subset of those clouds that produce surface precipitation live distinctly longer, on average 62 min in the standard RICO simulation and 48 min in the moist RICO simulation.

As expected, the largest clouds gain the highest rainwater mass through autoconversion, m_{au}, and produce the highest amount of surface precipitation, although the spread is found to be surprisingly large (Figures 2d and 2g). This means that the mean cloud volume is a first indicator of the accumulated autoconversion rate of cloud water to rainwater during a cloud's lifetime, and that the accumulated autoconversion rate is a first indicator of the surface precipitation, but both do not determine the surface precipitation fully. Despite m_{au} also the relative contribution of accretion compared to autoconversion (m_{accr}/m_{au}, Figures 2e and 2h) and the efficiency of a cloud to produce surface precipitation from rainwater (surface precipitation/($m_{au} + m_{accr}$), Figures 2f and 2i) increase with increasing cloud volume and increasing surface precipitation. Note that the precipitation efficiency shown in Figures 2f and 2i differs from the usual definition of the precipitation efficiency (i.e., the surface precipitation normalized by the time-integrated total condensate) [e.g., *Sui et al*., 2007; *Seifert and Stevens*, 2010].

For those clouds that do not produce surface precipitation, the rainwater mass gained through accretion is mostly smaller than the rainwater mass gained through autoconversion. Only for those clouds that produce surface precipitation, m_{accr}/m_{au} increases rapidly (Figure 2e). This confirms the increasing importance of accretion over autoconversion as precipitation rates increase, which has also been found, e.g., by *Gerber et al*. [2008], *Stevens and Seifert* [2008], and *Feingold et al*. [2013].

3.2. Lagrangian Drop Trajectory

A sample trajectory of an LD originating from the cloud that precipitates most in the moist RICO simulation and some properties of that cloud are shown in Figure 3. The LD originates near cloud top (at 158 min) where most raindrops form. After an initial ascent inside the cloud during which the LD's diameter increases, the LD is leaving the cloud near cloud top (at 164 min) and descends in the cloud environment, where some of its mass evaporates. Then, the LD reenters the cloud again (at 169 min), experiences a second updraft phase and a second period of growth. During this second period, the overall cloud volume and the cloud average cloud liquid water path start to decrease, while the average rainwater path of the projected cloud area increases. After a second height maximum, the LD leaves the cloud again well above cloud base (at 180 min) and some of its mass is evaporated while the LD is falling toward the subcloud layer and finally to the surface.

For the sample trajectory, the second updraft phase is essential for the overall growth of the LD and the simplified, conceptual picture of a raindrop that originates near cloud top, and then falls straight through the cloud and to the ground, is not valid in this case. We will show in the following that such an LD trajectory as outlined above with several height maxima and a last in-cloud height well above cloud base is typical in our simulations at least for a large portion of those raindrops that reach the surface.

3.3. Lagrangian Drop Statistics

While for the bulk rain microphysics scheme, physical processes such as sedimentation, evaporation, accretion, and selfcollection are parameterized in terms of an assumed RSD, in the LD model, those processes only depend on the individual LD's velocity and size, and its environmental conditions [*Naumann and Seifert*, 2015]. In the following, we will analyze the growth history of the LDs focusing on growth mechanisms that enable raindrops to reach the surface by comparing those LDs that reach the surface with those that evaporate before.

Most of the simulated LDs have a maximum diameter of less than 500 μm during their lifetime (Figure 4a) and evaporate completely when they leave the cloud. Only 1.2% of the LDs from the standard RICO simulation and

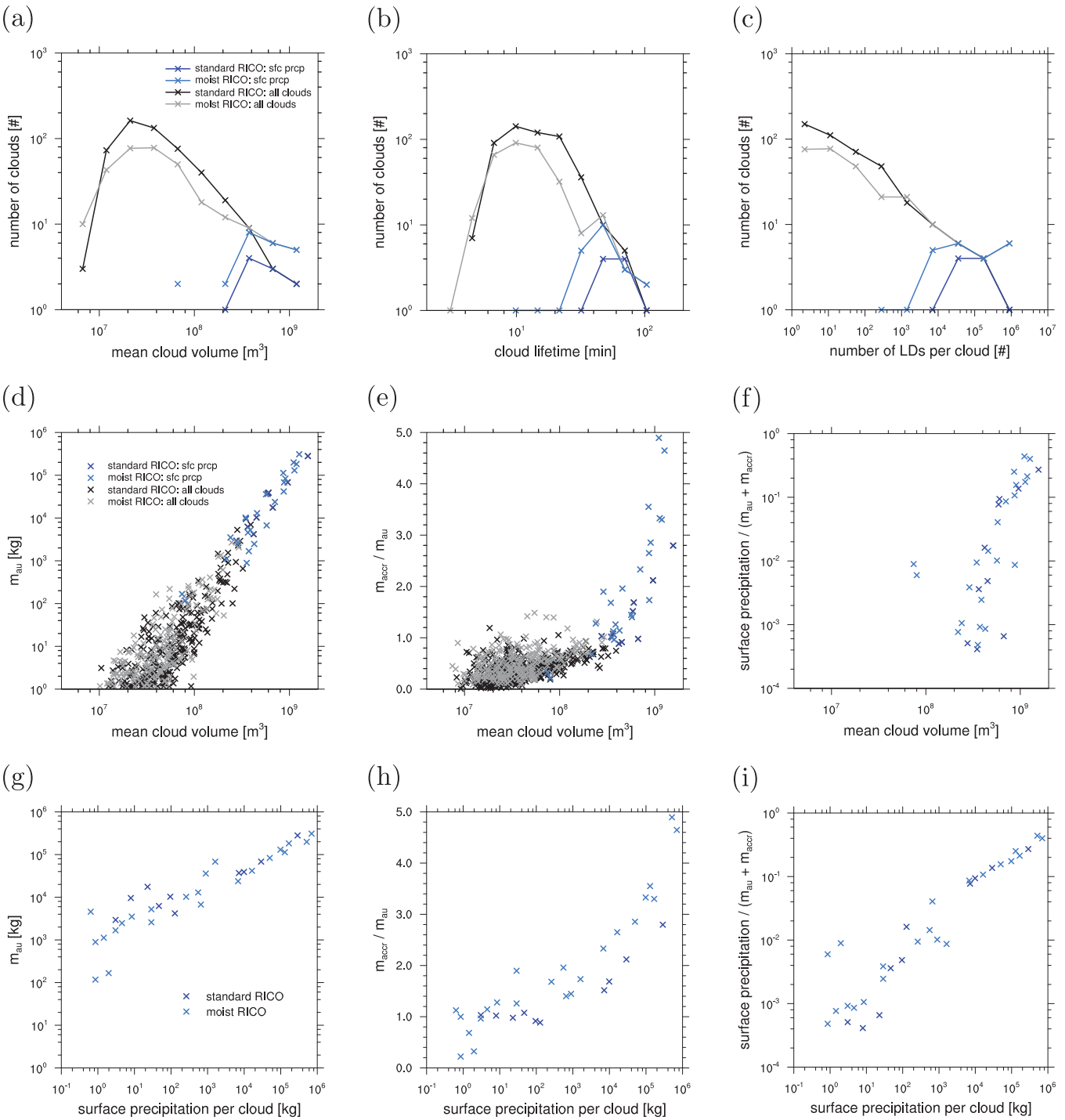

Figure 2. Cloud properties. All statistics are calculated only for active clouds and only for those LDs that are associated with exactly one active cloud. Shown are histograms (a) for the mean cloud volume, (b) for the cloud lifetime, and (c) for the number of LDs per cloud, and scatterplots (d–f) for the mean cloud volume and (g–i) for the amount of surface precipitation per cloud as a function of (d, g) the rainwater mass gained through autoconversion, m_{au}, (e, h) the relative contribution of accretion to autoconversion, m_{accr}/m_{au}, and (f, i) the efficiency of a cloud to produce surface precipitation from rainwater, surface precipitation/$(m_{au} + m_{accr})$. Note the logarithmic size binning in Figures 2a–2c.

3.1% from the moist RICO simulation become so large that they reach the surface before evaporating completely. All LDs with a maximum diameter larger than 600 μm in the standard RICO simulations and with a diameter larger than 640 μm in the moist RICO simulation contribute to surface precipitation. Because the number of LDs is decreasing rapidly with increasing diameter, for both simulations most of the surface precipitation mass originates

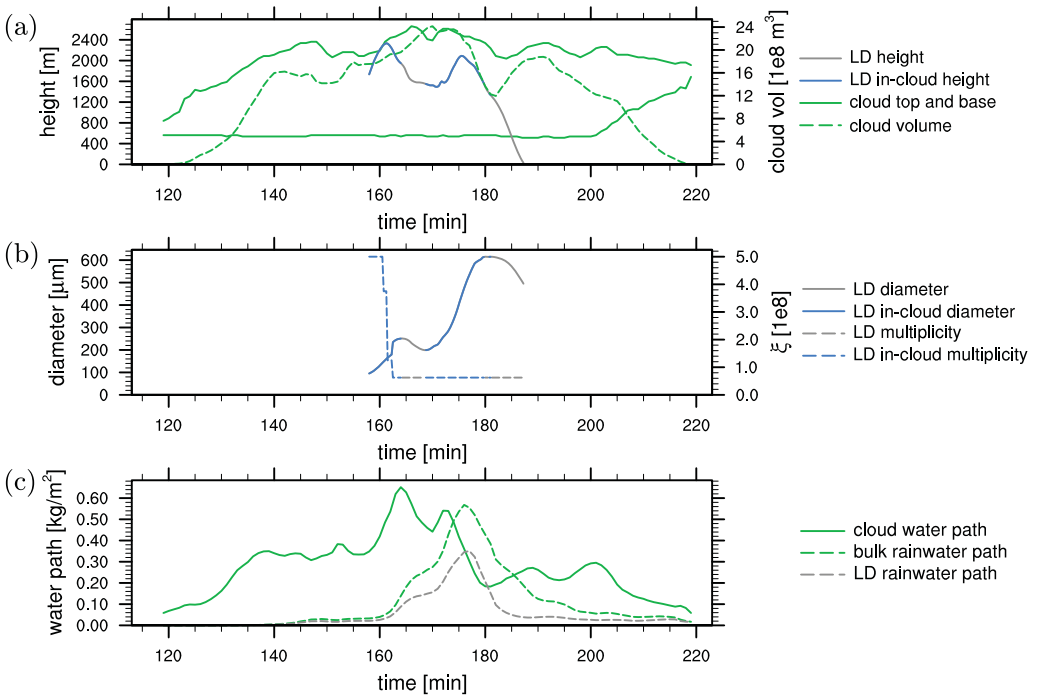

Figure 3. Sample trajectory of an LD that originates from the cloud that precipitates most in the moist RICO simulation. In addition, properties of that cloud are shown.

from rather small LDs with a diameter of less than 1.5 mm (72% of the surface precipitation mass for the standard RICO simulation, 74% for the moist RICO simulation, Figure 4d).

Somewhat counterintuitively, it is not the LDs with the longest lifetime that grow largest (Figure 4b, also Figures 7a and 7b). Only a few of the LDs live as long as 1 h, and most of the LDs have a lifetime of less than 10 min. Those that eventually contribute to surface precipitation mostly reach the surface about 20 min after their initialization. In general, a raindrop can grow the larger the longer it lives, but large raindrops also sediment faster than smaller raindrops, which prevents a long lifetime because the large raindrops reach the surface faster. Although the in-cloud residence time determines the time an LD can grow by accretion, also the in-cloud residence time is not a sufficient criterion for the largest LDs (Figure 4c) due to vastly different cloud water contents within a cloud. Note that the LD's lifetime and in-cloud residence time represent the raindrop phase only, i.e., it excludes a prior cloud droplet lifetime, which is not simulated with the LD model.

Compared to the average lifetime of a cloud that produces surface precipitation (50–60 min; Figure 2b), the average lifetime and in-cloud residence time of an LD that contributes to surface precipitation is distinctly shorter (20 min in Figure 4e and 15 min in Figure 4f, respectively). This difference is at least partly explained by the time that is needed for the broadening of the cloud droplet size distribution in the bulk microphysics scheme before the onset of autoconversion, i.e., the formation of raindrops.

The histograms of the LD's maximum diameter, its lifetime, and its in-cloud residence time are similar for the standard RICO simulation and the moist RICO simulation but some difference can be found in the details (Figure 4): for the moist RICO simulation, the surface precipitation is contributed from LDs with an average lifetime and an average in-cloud lifetime that is about 1 min shorter than for the standard RICO simulation (Figures 4e and 4f). We hypothesize that these small differences are related to a small shift in the relative importance of accretion and selfcollection, which we discuss in the following section.

4. Raindrop Growth

4.1. Accretion and Selfcollection

The mass gain of a raindrop by accretion can be quantified by [*Naumann and Seifert*, 2015, equation (7) therein]

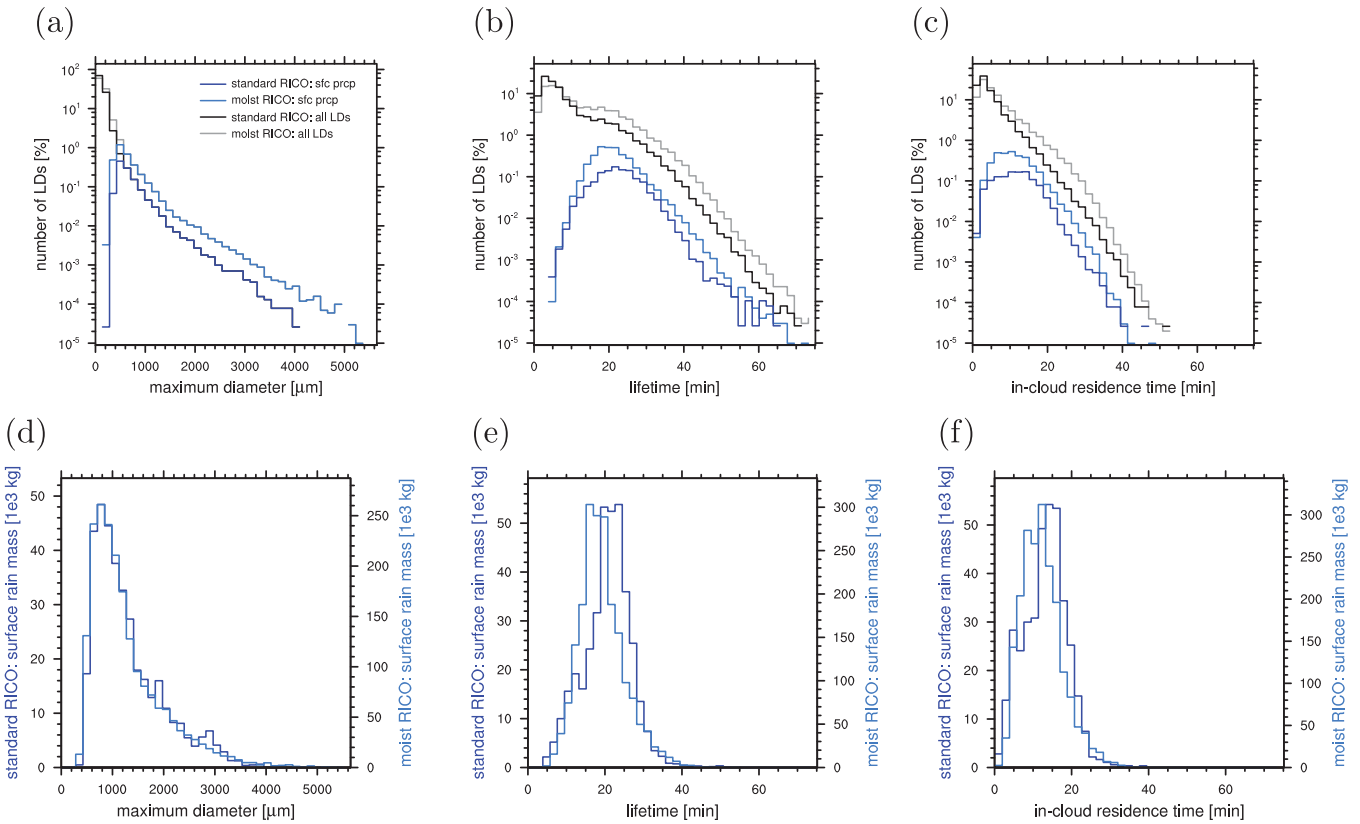

Figure 4. Histograms of LD properties (top row) in terms of the number of LDs and (bottom row) in terms of their contribution to surface precipitation mass.

$$\left.\frac{dm}{dt}\right|_{accr} = E_c \pi \rho_a r_{max}^2 |\vec{v}_d - \vec{v}_a| q_c \tag{1}$$

Assuming that an LD is growing only by accretion and is not evaporating, its mass evolution can be described as a function of the cloud liquid water mixing ratio, q_c, along the LD's trajectory. To derive an analytical expression for the LD's mass gain by accretion, we approximate the collision-coalescence efficiency, E_c, by unity, the air density, ρ_a, by the air density at a typical height for a raindrop, $\rho_{a,c} = 1.0$ kg/m^3 (at about 2000 m), the maximum dimension of the drop, r_{max}, by its mass equivalent radius, r, i.e., the radius of the mass equivalent perfect sphere, and the difference between the LD velocity and the ambient flow velocity, $|\vec{v}_d - \vec{v}_a|$, by the LD's terminal fall velocity, v_t. For small raindrops with 40 μm $< r <$ 600 μm, an approximation of the terminal fall velocity is $v_t = k_v r$, where $k_v = 8 \times 10^3$ s^{-1} [*Rogers and Yau*, 1989] (based on the data of *Gunn and Kinzer* [1949]). Then equation (1) simplifies to

$$\left.\frac{dm}{dt}\right|_{accr} = \pi \rho_{a,c} k_v r^3 q_c \tag{2}$$

Furthermore, r is related to the LD's mass, m, by $r^3 = 3/(4\pi\rho_w)m$, where ρ_w is the liquid water density. Integrating equation (2) results in

$$\ln\left(\frac{m_{accr}}{\overline{m}_0} + 1\right) = k_m Q_{c,LD} \quad \text{or} \tag{3}$$

$$\overline{r}_0 + r_{accr} = \overline{r}_0 \exp\left(k_r Q_{c,LD}\right) \tag{4}$$

where r_{accr} is the increase in LD radius due to accretion, $\overline{m}_0 = 3.9 \times 10^{-10}$ kg is the mean initial mass of an LD, and $\overline{r}_0 = 45.3$ μm is the corresponding mean initial mass equivalent radius of an LD. The factors k_m and k_r are $k_m = \frac{3\rho_{a,c}}{4\rho_w} k_v = 6.0\,\text{s}^{-1}$ and $k_r = \frac{1}{3} k_m$. The integral cloud water along the LD's trajectory, $Q_{c,LD}$, has been discussed by *Feingold et al.* [2013] as a precipitation-controlling parameter and is defined as

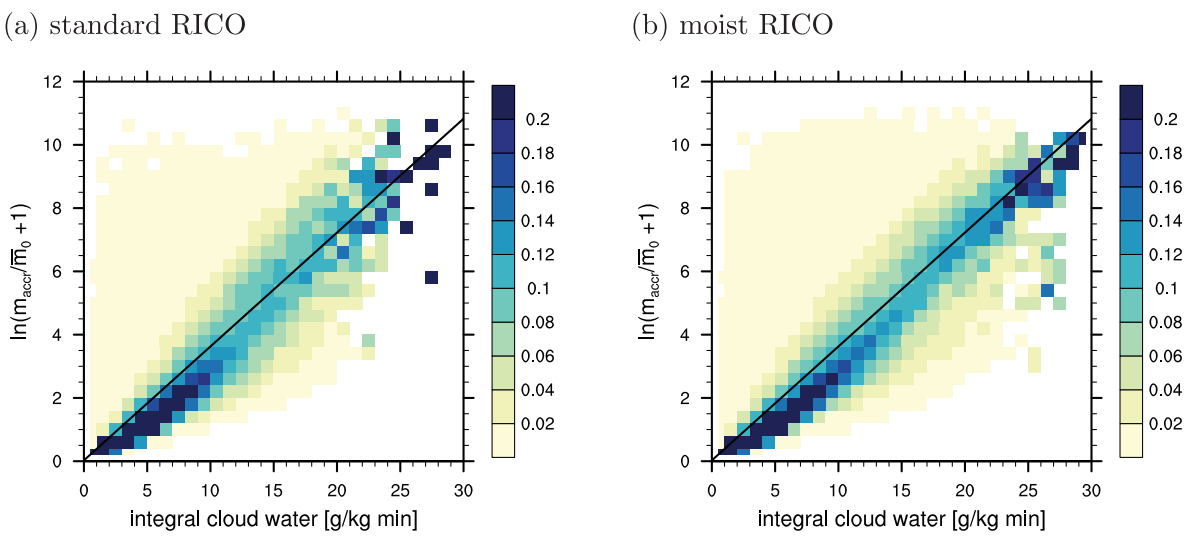

Figure 5. Raindrop mass growth by accretion: PDF of $\ln(m_{\mathrm{accr}}/\overline{m}_0+1)$ as a function of the integral cloud water, $Q_{c,\mathrm{LD}}$. The solid line shows the relation from equation (3).

$$Q_{c,\mathrm{LD}} = \int_{t_0}^{t_1} q_c(\vec{x})\,\mathrm{d}t \tag{5}$$

where q_c is integrated over the lifetime of the LD from t_0 to t_1 and $\vec{x}$ is the LD's position.

In Figure 5, the LDs' mass gain by accretion is shown as a function of $Q_{c,\mathrm{LD}}$ together with the relation from equation (3). For small $Q_{c,\mathrm{LD}}$, the LD growth is slightly smaller than the analytical relation. This overestimation by the analytical relation is (at least partly) caused by the assumed dependence of v_t on r, which overestimates v_t slightly for small raindrops. Overall, $Q_{c,\mathrm{LD}}$ is a good measure for the LD's mass gain through accretion. Consistently, for the standard and the moist RICO simulation, all LDs that experience a large $Q_{c,\mathrm{LD}} > 20$ g/kg min eventually contribute to surface precipitation (Figures 6a and 6d).

In addition to accretion, an LD's mass also grows by selfcollection. The growth rate by selfcollection is independent of the cloud water content but depends on the LD's properties and on the number density of LDs in the vicinity of that LD. The probability of selfcollection for an LD pair is proportional to the square of the sum of the LDs' radii and to the velocity difference of the LDs [*Naumann and Seifert*, 2015, equation (13) therein]. Whether two LDs, that have a certain probability to collide, do collide in the LD model is determined by Monte-Carlo sampling. Therefore, for a population of LDs, the growth rate by selfcollection depends on the drop size and the number density of the LDs. However, whether (and how much) a single LD grows by selfcollection also depends on a random number process and therefore on luck. This dependence on luck is in line with our understanding of a real single raindrop's growth.

Normalizing the LD growth through accretion by the maximum mass of the LD during its lifetime, two groups are found for those LDs that contribute to surface precipitation (Figures 6b and 6e): the first group of LDs with values around one gains mass mainly through accretion. The normalized LD growth through accretion can be larger than one if some of the LD's mass is evaporated before new mass is gained again through accretion. The second group with values close to zero dominantly grows from selfcollection. The accretion-dominated LDs and the selfcollection-dominated LDs seem to contribute about the same amount to the overall surface rain mass for the moist RICO simulation. For the standard RICO simulation, a slight shift to the accretion-dominated LDs can be found. If the maximum mass is small, the initial mass contributes a large portion to the maximum mass. Because most of the LDs have such a small maximum mass, this explains the relatively broad maximum at low values when all LDs are considered.

For most of those LDs that contribute to surface precipitation, growth predominantly takes place in updraft regions (Figures 6c and 6f). In a cloud, liquid water forms in the updraft region and therefore growth through accretion is effective there. However, there is a second peak that contributes to surface precipitation, where LDs only gain a small fraction of their mass in updraft conditions. Here the individual LDs mostly grow from selfcollection.

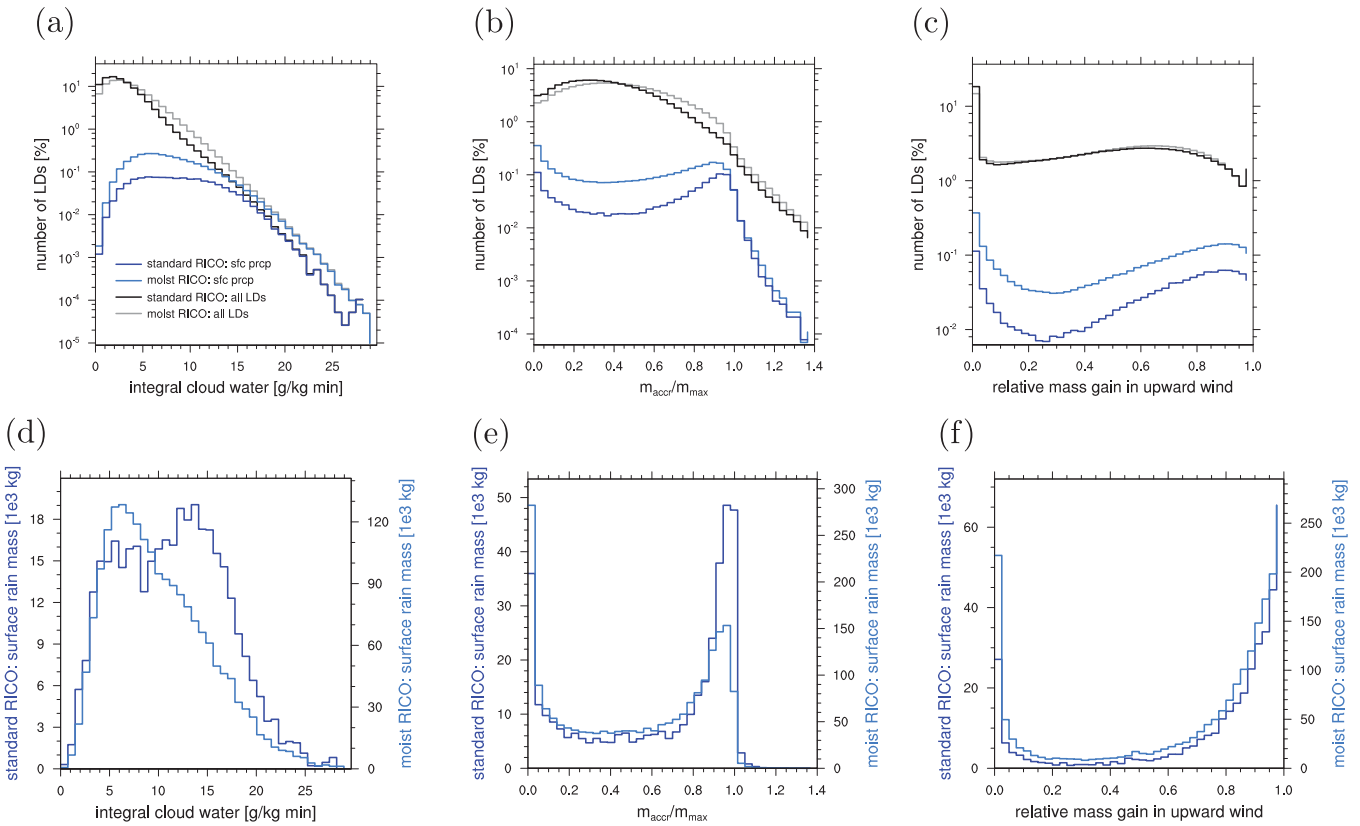

Figure 6. Histograms of LD properties (top row) in terms of the number of LDs and (bottom row) in terms of their contribution to surface precipitation mass.

The two branches found for the LD lifetime and the integral cloud water for the standard RICO simulation are also associated with the two growth regimes (Figures 7a and 7c). For pure accretional growth, the maximum diameter increases with integral cloud water. Because selfcollection is independent of the integral cloud water, a second branch with low integral cloud water is found for all LD sizes. A corresponding two-branch behavior can be found for the LD's lifetime. If selfcollection becomes more important for the growth rate, the LD's lifetime can be distinctly reduced. For the moist RICO simulation, the two branches cannot be found and the integral cloud water displays the increasing importance of selfcollection compared to the standard RICO simulation (Figures 7b and 7d).

Having identified the two growth regimes from an individual LD's perspective, we now focus on the relative importance of accretion and selfcollection for the development of the whole RSD. For a given RSD, the change in the mean raindrop mass, $\overline{m}=q_r/n_r$, can be characterized by the change in rainwater mixing ratio, q_r, and the change in raindrop number density, n_r:

$$\frac{\partial \overline{m}}{\partial t}=\frac{\partial}{\partial t}\left(\frac{q_r}{n_r}\right)=\frac{1}{n_r}\frac{\partial q_r}{\partial t}-\frac{q_r}{n_r^2}\frac{\partial n_r}{\partial t} \tag{6}$$

Accretion is changing q_r while n_r stays constant. Vice versa, selfcollection is changing n_r while q_r stays constant.

$$\left.\frac{\partial \overline{m}}{\partial t}\right|_{\text{accr}}=\left.\frac{1}{n_r}\frac{\partial q_r}{\partial t}\right|_{\text{accr}}=\frac{1}{n_r}k_r q_c q_r \phi_{\text{accr}}(\tau) \tag{7}$$

$$\left.\frac{\partial \overline{m}}{\partial t}\right|_{\text{sc}}=-\left.\frac{q_r}{n_r^2}\frac{\partial n_r}{\partial t}\right|_{\text{sc}}=\frac{q_r}{n_r^2}k_r n_r q_r \tag{8}$$

where the second equality is obtained by using the parameterization for accretion and selfcollection from *Seifert and Beheng* [2001]. The universal function ϕ_{accr} provides a considerable contribution only for very small $\tau=1-q_c/(q_c+q_r)$. With that parameterization, the ratio, $f_{\overline{m}}$, of the mean raindrops mass gain through

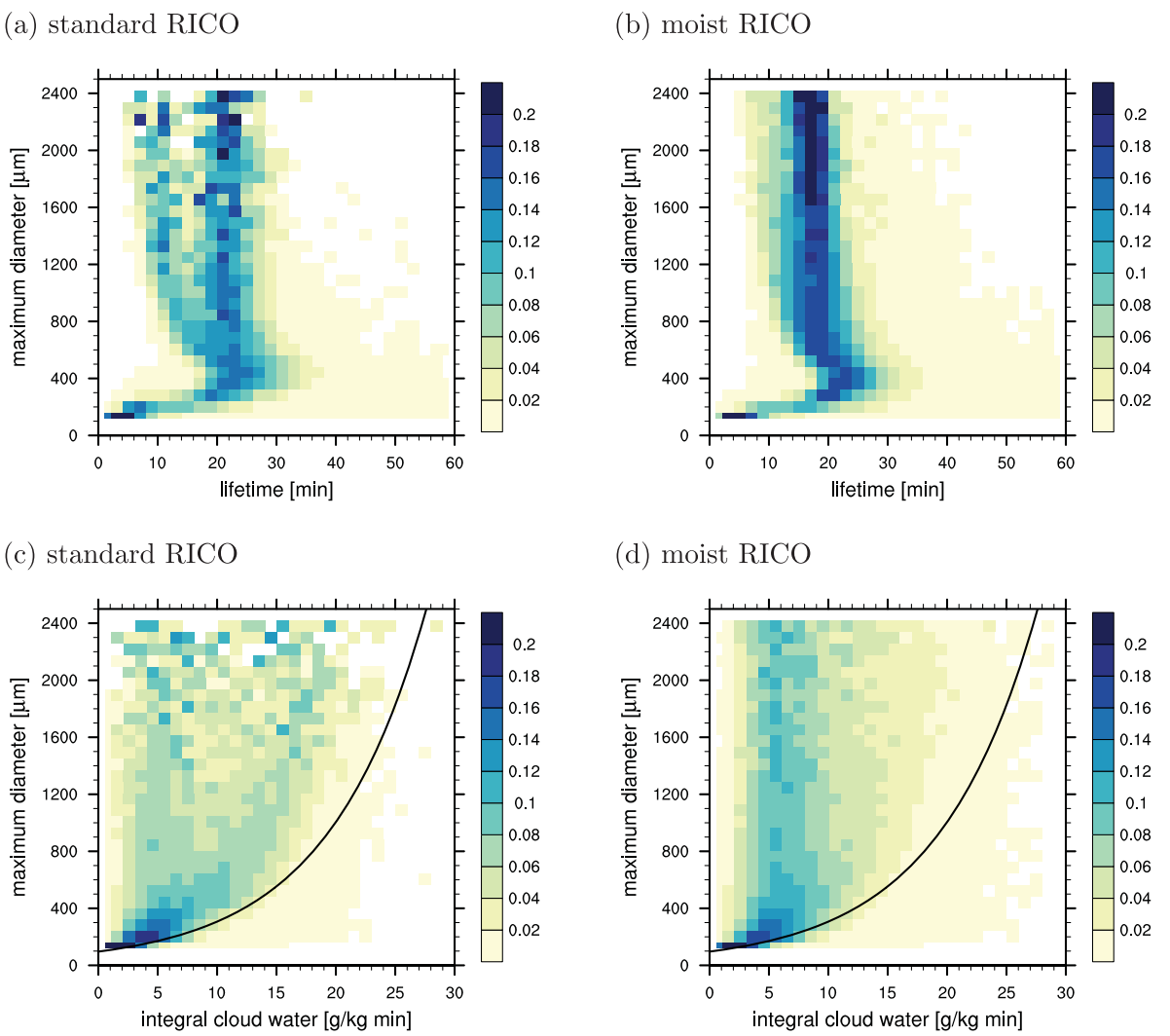

Figure 7. PDFs of the lifetime and of the integral cloud water as a function of the maximum diameter. The solid line in Figures 7c and 7d shows the relation of equation (4), i.e., how the maximum diameter relates to the integral cloud water if solely accretion was considered.

accretion to the mean raindrop mass gain through selfcollection can be expressed as the ratio of the cloud water mixing ratio to the rainwater mixing ratio:

$$f_{\overline{m}} = \frac{\frac{\partial \overline{m}}{\partial t}|_{\text{accr}}}{\frac{\partial \overline{m}}{\partial t}|_{\text{sc}}} = \frac{q_c}{q_r}\phi_{\text{accr}}(\tau) \tag{9}$$

Figure 8 shows the temporal development of the cloud mean values of q_c and q_r for those two clouds that produce most surface precipitation in the standard and the moist RICO simulation. For both clouds, q_c increases rapidly when the cloud is forming. Then, as autoconversion and accretion set in, q_r increases at the expense of q_c. At the end of a cloud's lifecycle, both q_c and q_r decrease and the cloud disappears. For the cloud from the standard RICO simulation, q_r is always smaller than q_c, i.e., $f_{\overline{m}}$ is always >1. For the moist RICO cloud for about 5 min, $f_{\overline{m}} < 1$, i.e., $q_r > q_c$ (compare with Figure 3c). Although local values at an LD's position may deviate substantially from cloud mean values and selfcollection may also take place outside the cloud, this confirms the more important role of selfcollection in the moist RICO simulation compared to the standard simulation.

4.2. The Role of Recirculation

After discussing the microphysical processes of raindrop growth in the previous section, we now focus on the dynamical aspects of a raindrop's lifecycle. Similar to the LD trajectory shown in Figure 3, many of the LDs and in particular those LDs that eventually reach the surface are found to *recirculate* in the cloud layer, i.e., many LDs do

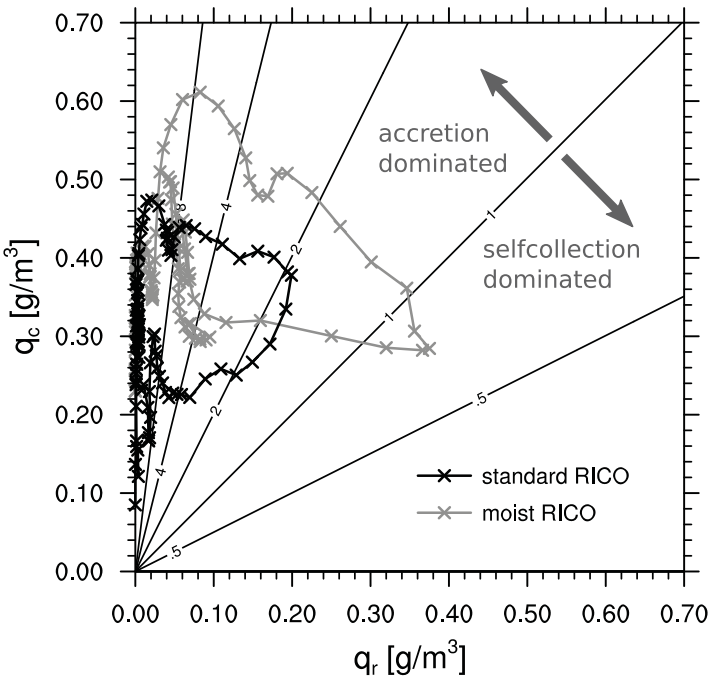

Figure 8. Ratio $f\overline{m}$ according to equation (9) as a function of q_c and q_r (labeled lines). Cloud mean values of q_c and q_r are shown for two selected clouds: those two clouds that form the most surface precipitation in the standard RICO simulation and in the moist RICO simulation. The temporal resolution for the mean cloud values is 1 min and the temporal development is in clockwise direction for both clouds.

not fall straight toward the surface but leave and reenter a cloud, and experience several height maxima during their lifetime. To analyze the *recirculation* of an LD in a quantitative way, we formulate two definitions of recirculation, one highlighting the horizontal displacement of an LD and one highlighting the vertical displacement of an LD:

Cloud-Edge Recirculation. An LD is recirculating if during its lifetime it is undergoing the consecutive events of being outside the cloud, having a height maximum within the cloud and being outside the cloud again.

200-m Recirculation. An LD is recirculating if during its lifetime it is undergoing consecutive periods of descent and ascent, each time achieving a height difference of at least 200 m.

The two definitions of recirculation do not exclude each other and one LD may undergo several recirculations of each type during its lifetime. For the first definition, the criterium of a height maximum within the cloud is chosen to exclude events where an LD just falls through a low level cloud fringe or wiggles back and forth on a cloud border. For the second definition, the threshold of 200 m for the minimum height difference is chosen because a threshold should be reasonably small to include most recirculations but at the same time should be considerably larger than the vertical grid spacing of 25 m. For the LD in Figure 3, these definitions yield one cloud-edge recirculation and one 200-m recirculation, both referring to the height maximum between 170 and 180 min.

In addition, we define updraft hopping:

Updraft Hopping. An LD is hopping between updrafts if during its lifetime it is found inside two different active clouds, i.e., during its lifetime, an LD is switching from the cloudy area that is attributed to one cloud core to the cloudy area that is attributed to another cloud core.

The two active clouds an LD is found in might be single clouds or parts of a multicore cloud system. Defining updraft hopping as switching between cloud cores instead of clouds would be an even more restrictive conditions, which is not applied here.

Table 2. Percentage of LDs that Recirculate or Hop Between Updrafts at Least Once[a]

	All LDs		sfc prcp LDs	
% RICO Simulation	Standard	Moist	Standard	Moist
Cloud-edge recirculation	13	16	66	47
200-m recirculation	3	4	38	22
Updraft hopping	2	2	1	1

[a]sfc prcp LDs—surface precipitating LDs, i.e., considering only those LDs that eventually contribute to surface precipitation.

For both definitions of recirculation, we find that considering all LDs the majority of LDs does not recirculate (Table 2) and that the percentage of LDs that recirculate is decreasing steadily with increasing number of recirculations at a very similar rate for the standard and the moist RICO simulation (Figures 9a and 9b). In contrast, for the subsample of those LDs that eventually reach the

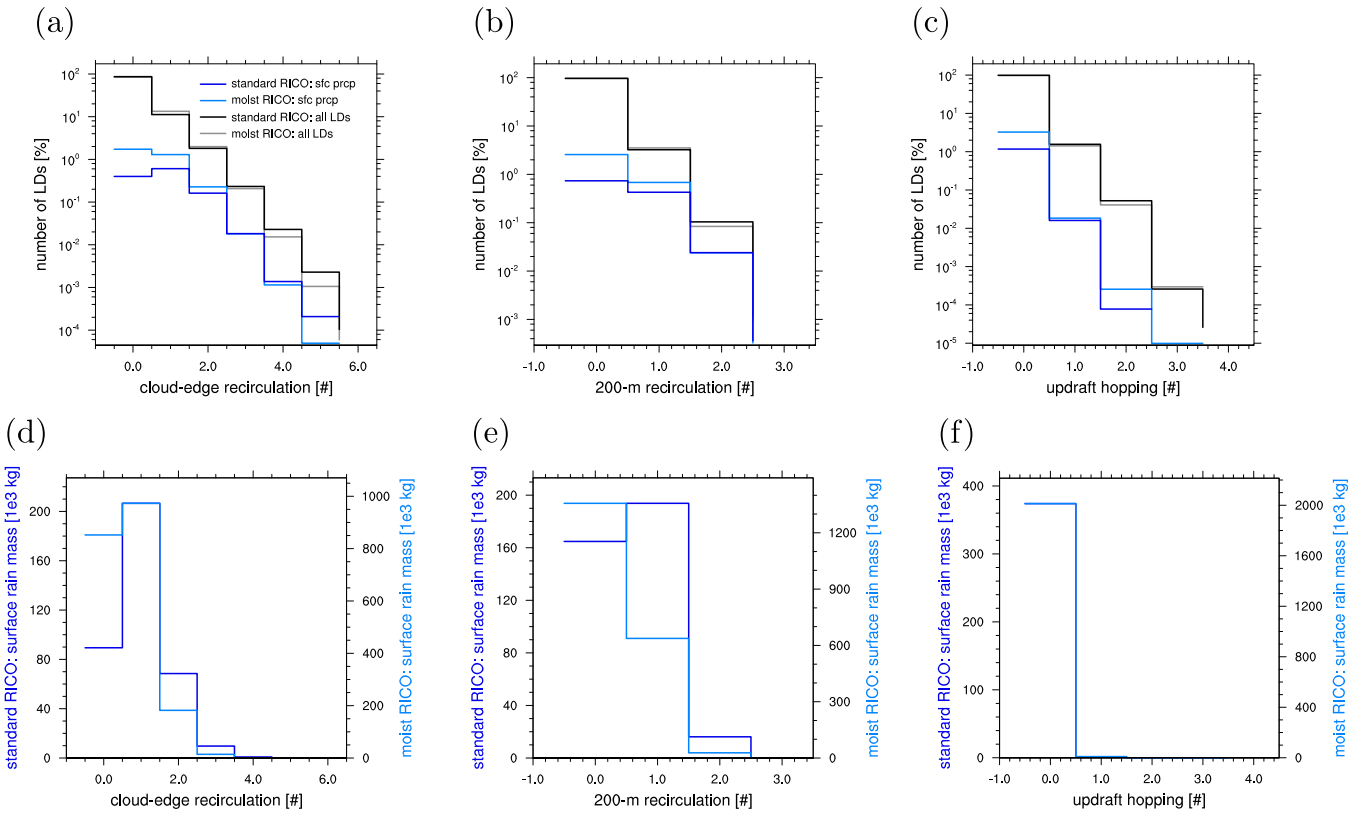

Figure 9. Histograms of LD properties (top row) in terms of the number of LDs and (bottom row) in terms of their contribution to surface precipitation mass.

surface and for the cloud-edge recirculation, about as many LDs do not recirculate as recirculate at least once (Figure 9a). For both RICO simulations, those LDs that experience at least one cloud-edge recirculation contribute more to the surface rain mass than those that do not recirculate, though the difference is larger for the standard RICO simulation (Figure 9d). For the 200-m recirculation, the statistics are similar, albeit high numbers of recirculation are less common (Figure 9b). For the moist RICO simulation, LDs that do not experience a 200-m recirculation contribute more mass to surface precipitation than those that recirculate once or more often (Figure 9e). The precise numbers differ depending on the definition of recirculation but overall we find that recirculation of raindrops is common in shallow cumulus, especially for those LDs that contribute to surface precipitation.

Applying the cloud tracking, we find that most of the LDs stay in the cloudy updraft region they originate from and do not hop between updrafts, regardless if they contribute to surface precipitation or evaporate before they reach the surface (Table 2 and Figure 9c). This also holds in terms of surface precipitation mass, i.e., those few LDs that make it to a second cloud do not contribute distinctly to the surface precipitation (Figure 9f).

The dynamical aspects of an LD's trajectory can be further characterized by relating the LD's position and flow properties to the cloud it originates from. During a cloud-edge recirculation event, the LDs depart from the cloud. For most of the LDs, the mean distance to the cloud-edge during a cloud-edge recirculation event is less than 50 m for the period that the LD is outside the cloud (Figure 10a). The portion of LDs is decreasing rapidly with increasing mean distance to the cloud-edge. Nevertheless, LDs with mean distances up to 200 m contribute to surface precipitation (Figure 10c).

While most of the LDs originate near cloud top between 2000 and 2500 m, the last in-cloud height for most of the LDs is only a couple of hundred meters lower (Figure 10b). For the subset of LDs that eventually contribute to surface precipitation, the last in-cloud height is typically about 1000 m below their initial height, around 1000 m for the standard RICO simulation and around 1400 m for the moist RICO simulation (Figure 10d). Only few LDs leave the cloud through cloud base, which for both simulations is at 600 m and increases for individual clouds toward the end of their lifetime when the cloud dissipates (e.g., Figure 3a).

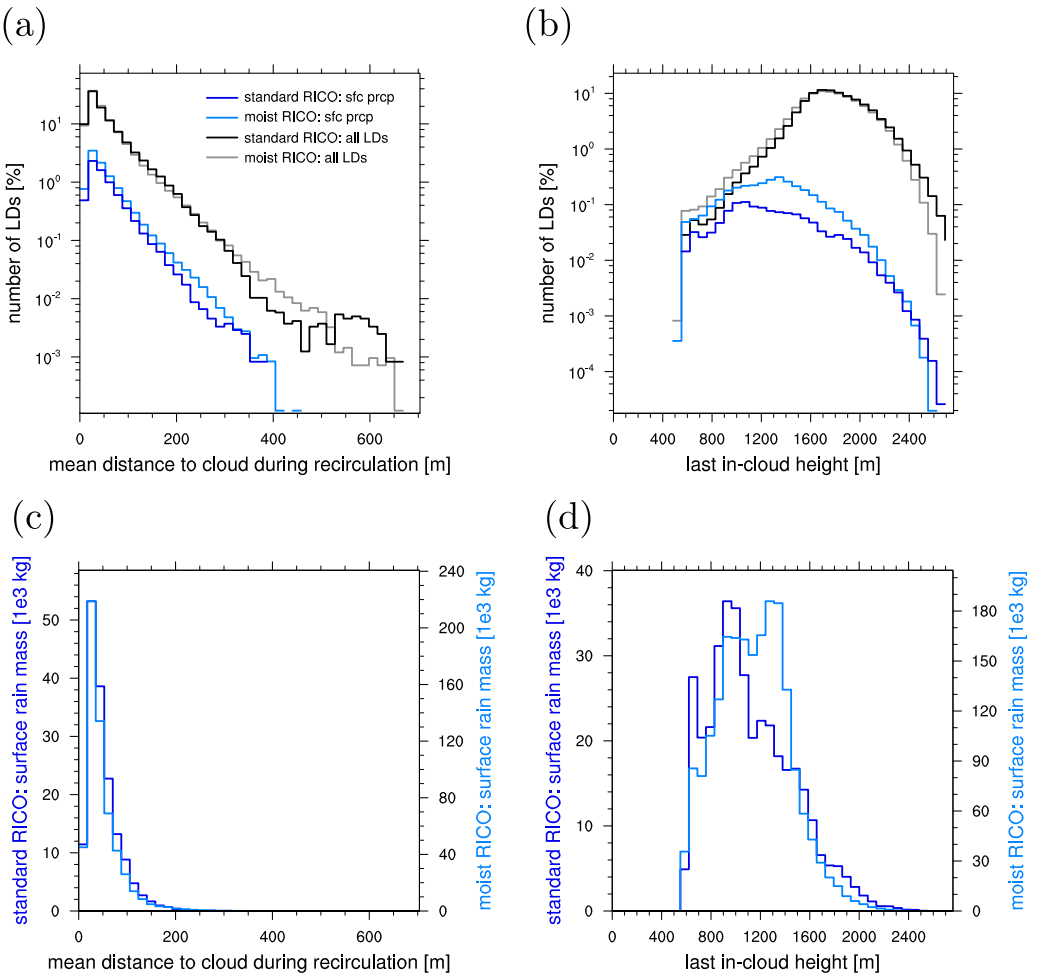

Figure 10. Histograms of LD properties (top row) in terms of the number of LDs and (bottom row) in terms of their contribution to surface precipitation mass.

That most LDs leave the cloud laterally and that a portion of them is able to reenter the cloud suggest that the LD motion is not bound to the cloud structure. The notion of an LD that resides in a cloud-core updraft like in an elevator and ascends and descends as the core is pulsating in strength is therefore not a reasonable explanation of the observed LD recirculation. The vertical velocity of the sample LD trajectory (introduced in Figure 3) is clearly more variable in time than the in-cloud vertical velocity averaged either over the cloud area or over the core area (Figure 11). Also, the vertical velocity of the sample LD trajectory does not agree well with the tendencies, the maxima, or the minima of these averaged velocities (Figure 11). The recirculation of LDs is therefore not directly related to the pulsating growth of the cloud as a whole [*Heus et al.*, 2009]. For both RICO simulations, the LD diameter increases with increasing in-cloud TKE along the LD

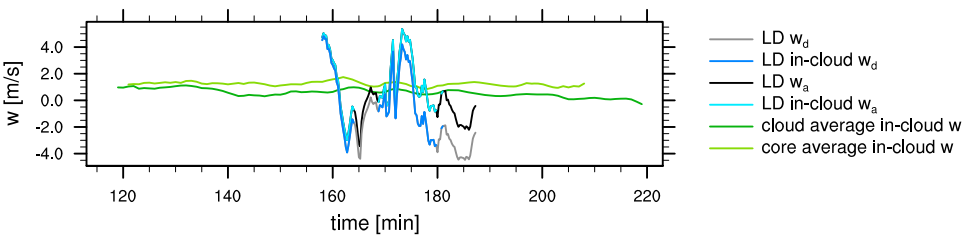

Figure 11. Vertical velocities for the sample trajectory in Figure 3. Shown are the LD's vertical velocity, w_d, the vertical flow velocity at the LD's position, w_a, and the column average in-cloud vertical velocity, w, averaged over the cloud area or the core area.

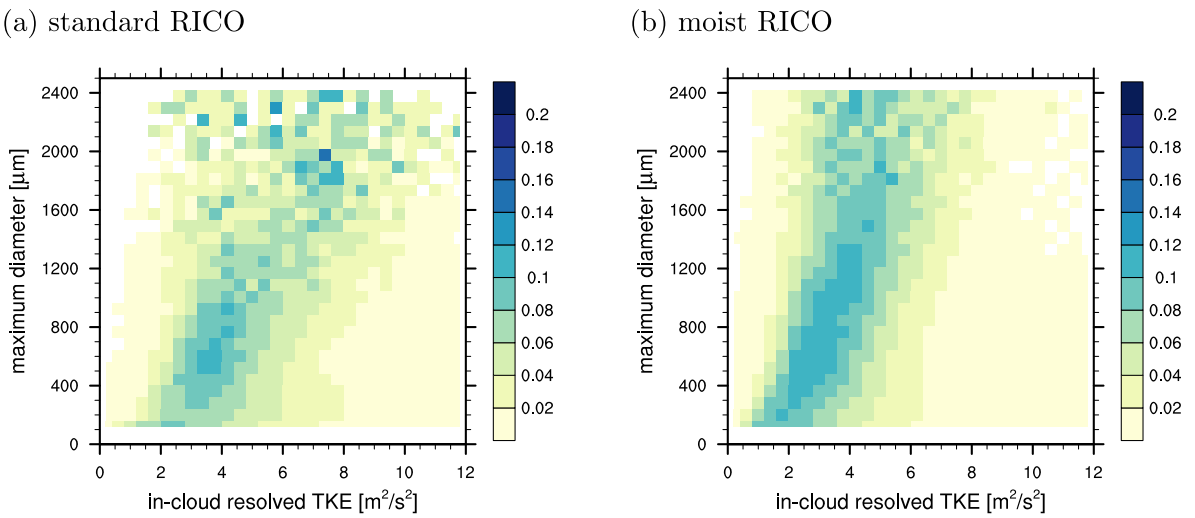

Figure 12. PDFs of the in-cloud resolved TKE along the LD's trajectory as a function of the maximum diameter.

trajectory (Figure 12). This suggests that the LDs are able to switch between different updraft structures on the subcloud scale, and that it is not the mean cloud properties alone that determine the raindrops growth but that the in-cloud variability is crucial.

Finding that recirculation is common, it is interesting to analyze how much of the surface precipitation a cloud is producing is actually contributed from those LDs that recirculate and how much those LDs grow during recirculation. To approach these questions, we estimate an upper bound and a lower bound of the surface precipitation contributed by recirculating LDs and compare it to the total precipitation. To estimate an upper bound, we sum the contribution to surface precipitation from that subsample of LDs that recirculate. However, those LDs that recirculate may be large enough to contribute to surface precipitation already before the (first) recirculation event sets in. To estimate a lower bound, we therefore subtract from the upper bound estimate the mass of those LDs that recirculate at the moment when they reach the last height minimum before the recirculation event. This lower estimate is not strictly the lowest bound because without a recirculation a raindrop could still grow while falling further through the cloud if the height minimum is inside a cloud. We expect this growth effect to be very small because the descent before the recirculation is often outside the cloud (Figure 9) and because as the last in-cloud height is rarely close to cloud base the potential growth path is short (Figure 10). In addition, evaporation in the cloud environmental air and in the subcloud layer, which is not considered in the estimate, decreases the LD's mass rather than increasing it.

Using those estimates for the upper and the lower bound, we find that the difference between the upper and lower bound for most clouds is much smaller than the difference between different clouds (Figure 13). For the cloud-edge recirculation, the contribution of the recirculating LDs to the surface precipitation is slightly higher than for the 200-m recirculation, which is reasonable because the cloud-edge recirculation is more frequent. For both definitions of recirculation and especially for the moist RICO simulation, the surface precipitation amount per cloud is the higher, the higher the contribution of the recirculating LDs is. For the most precipitating clouds, the LDs that recirculate can contribute more than 50% to the total surface precipitation (Figure 13d). For the whole cloud field, the contribution of recirculating LDs to the overall surface precipitation rate is dominated by those clouds that produce the highest amount of surface precipitation (Figures 13a and 13b): for the standard RICO simulation, the contribution of the recirculating raindrops to the total surface precipitation is 72% for the cloud-edge recirculation and 54% for the 200-m recirculation; for the moist RICO simulation, it is 53% for the cloud-edge recirculation and 31% for the 200-m recirculation. This implies that coarse resolution models that do not resolve those eddies that cause recirculation of raindrops omit a relevant process of rain formation in shallow cumulus. The importance of recirculation and small eddies are a possible explanation for the slow convergence of LES for precipitating shallow convection found by *Matheou et al.* [2011].

Comparing both RICO simulations, the contribution of recirculating LDs to the total surface precipitation is smaller for the moist RICO simulation (Figures 13c and 13d), which is characterized by a higher mean

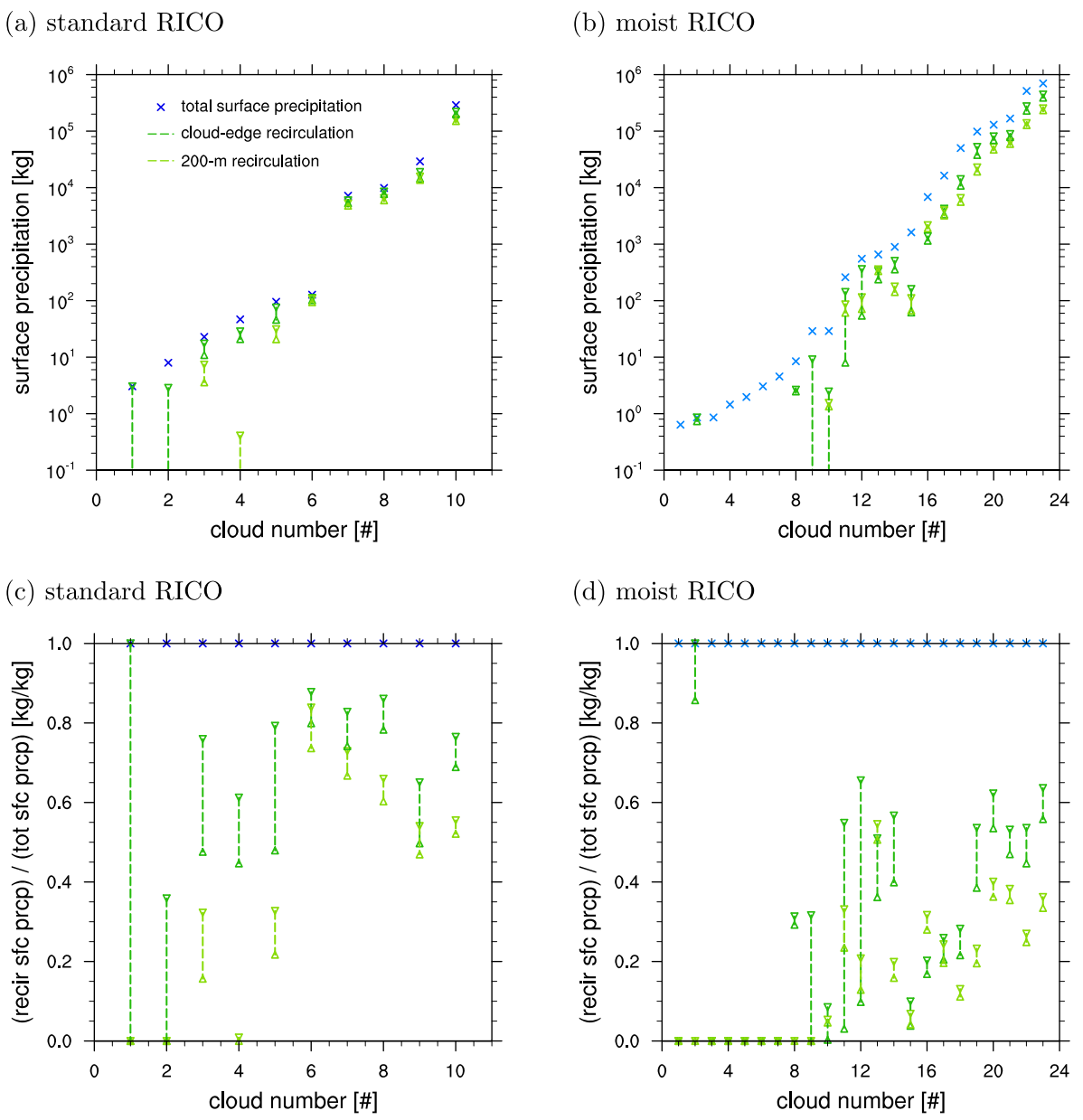

Figure 13. Total surface precipitation per cloud and relative contribution of recirculating LDs to the total precipitation per cloud. Triangle top down: upper bound, i.e., contribution to surface precipitation only by those LDs that recirculate. Triangle top up: lower bound, i.e., surface precipitation by those LDs that recirculate minus the mass of those LDs that recirculate at their height minimum before the recirculation.

surface precipitation rate than the standard RICO simulation (Table 1). This is somewhat surprising because, as discussed above, the contribution of recirculating LDs to the total surface precipitating per cloud is increasing with increasing surface precipitation per cloud. We speculate that the smaller contribution for the moist RICO simulation is related to the larger relative contribution of selfcollection compared to accretion for the moist RICO simulation and the slightly longer LD lifetime for the standard RICO case.

For a parameterization of the effect of recirculation, a relation of the contribution of the recirculating raindrops to some model parameter is needed. We find no hint for such a relation for the spatial extent of the cloud, e.g., for the cloud height or the cloud volume, which might be related to the rather small cloud height differences in the simulations. But the contribution of the recirculating raindrops to the overall precipitation roughly increases with increasing cloud lifetime and with increasing maximum of the column average in-cloud vertical velocity for the moist RICO simulation (not shown). For the standard RICO

simulation, these relations are less clear. The development of a parameterization that takes into account the effect of recirculation needs further investigation but a relation to cloud lifetime or to cloud updraft strength seems to be a useful starting point.

5. Conclusions

In this study, growth histories of raindrops in lightly precipitating shallow cumulus fields are investigated. Two related cases of fields of shallow cumulus are simulated using an LES combined with an LD model for raindrop growth and a cloud tracking algorithm. Overall, 1.4×10^7 LDs are simulated and more than 800 clouds are tracked of which 33 produce surface precipitation. We find that a first estimate of the amount of surface precipitation per cloud can be inferred from the accumulated autoconversion rate during a cloud's lifetime but the accumulated autoconversion rate does not determine the surface precipitation fully. Instead, we find considerable spread among individual clouds.

In our simulations, 1%–3% of the LDs but all of those with a maximum diameter larger than 640 μm reach the ground as surface precipitation. Most of the LDs have a lifetime of less than 10 min. The subsample of those LDs that contribute to surface precipitation live considerably longer, on average about 20 min. The largest LDs do not have the longest lifetime or longest in-cloud residence time because larger raindrops sediment faster and therefore also reach the ground faster.

Two processes determine raindrop growth: accretion of bulk cloud water and selfcollection among raindrops. For the standard RICO simulation, the two regimes can be clearly identified: in the first regime, growth is dominated by accretional growth and the size of the LDs is closely related to the integral cloud water along their trajectory. In the second regime, selfcollection has a more important role, the size of the LDs is independent of the integral cloud water and the LDs have a shorter lifetime compared to the accretional growth regime.

We find that raindrop trajectories in shallow cumulus can be quite complex. The LDs typically leave the cloud well above cloud base, and a substantial part especially of those LDs that contribute to surface precipitation leave and then reenter the same cloud for an additional updraft period. Accordingly, those trajectories often feature several height maxima, and the LD properties are less influenced by cloud-mean properties but the in-cloud variability is crucial. Because LDs with very different growth histories can be located in close vicinity, the diversity of LD trajectories contributes to RSD broadening.

The fraction of surface precipitation that can be attributed to recirculating LDs is variable from cloud to cloud but seems to increase with increasing surface precipitation amount and can be larger than 50% per cloud. This implies that the traditional, conceptual picture of a raindrop that originates near cloud top, that then gains mass while it falls straight through the cloud without any recirculation and that finally leaves the cloud at cloud base falling further to the ground, is too simplified especially for those raindrops that eventually contribute to surface precipitation. Highly idealized one-dimensional models of rain formation that neglect the recirculation of raindrops and models with coarse resolution that do not resolve those eddies that cause recirculation of raindrops therefore omit a relevant process that contributes distinctly to surface precipitation.

Acknowledgments
We thank Alberto de Lozar, Cathy Hohenegger, and two anonymous reviewers for their valuable comments, which helped to improve the manuscript. The source code of UCLA-LES including the extension of the LD model and the cloud tracking algorithm is released under the GNU General Public License and is publicly available on github (https://github.com/uclales/). Primary data and scripts used in the analysis and other supporting information that may be useful in reproducing the author's work are archived by the Max Planck Institute for Meteorology and can be obtained by contacting publications@mpimet.mpg.de. This research was carried out as part of the Hans-Ertel Centre for Weather Research. This research network of Universities, Research Institutes, and the Deutscher Wetterdienst is funded by the BMVI (Federal Ministry of Transport and Digital Infrastructure).

References

Andrejczuk, M., W. W. Grabowski, J. Reisner, and A. Gadian (2010), Cloud-aerosol interactions for boundary layer stratocumulus in the Lagrangian cloud model, *J. Geophys. Res.*, *115*, D22214, doi:10.1029/2010JD014248.

Bewley, J. L., and S. Lasher-Trapp (2011), Progress on predicting the breadth of droplet size distributions observed in small cumuli, *J. Atmos. Sci.*, *68*(12), 2921–2929, doi:10.1175/JAS-D-11-0153.1.

Browning, K., and G. Foote (1976), Airflow and hail growth in supercell storms and some implications for hail suppression, *Q. J. R. Meteorol. Soc.*, *102*(433), 499–533.

Browning, K. A. (1964), Airflow and precipitation trajectories within severe local storms which travel to the right of the winds, *J. Atmos. Sci.*, *21*, 634–639.

Chosson, F., P. A. Vaillancourt, J. A. Milbrandt, M. Yau, and A. Zadra (2014), Adapting two-moment microphysics schemes across model resolutions: Subgrid cloud and precipitation fraction and microphysical sub–time step, *J. Atmos. Sci.*, *71*(7), 2635–2653.

Cooper, W. A. (1989), Effects of variable droplet growth histories on droplet size distributions. Part I: Theory, *J. Atmos. Sci.*, *46*(10), 1301–1311.

Cooper, W. A., S. G. Lasher-Trapp, and A. M. Blyth (2013), The influence of entrainment and mixing on the initial formation of rain in a warm cumulus cloud, *J. Atmos. Sci.*, *70*(6), 1727–1743.

Devenish, B., et al. (2012), Droplet growth in warm turbulent clouds, *Q. J. R. Meteorol. Soc.*, *138*(667), 1401–1429.

Feingold, G., B. Stevens, W. R. Cotton, and A. S. Frisch (1996), The relationship between drop in-cloud residence time and drizzle production in numerically simulated stratocumulus clouds, *J. Atmos. Sci.*, *53*, 1108–1122.
Feingold, G., A. McComiskey, D. Rosenfeld, and A. Sorooshian (2013), On the relationship between cloud contact time and precipitation susceptibility to aerosol, *J. Geophys. Res. Atmos.*, *118*, 10,544–10,554, doi:10.1002/jgrd.50819.
Gerber, H. E., G. M. Frick, J. B. Jensen, and J. G. Hudson (2008), Entrainment, mixing, and microphysics in trade-wind cumulus, *J. Meteorol. Soc. Jpn.*, *86*, 87–106.
Grabowski, W. W., and L.-P. Wang (2013), Growth of cloud droplets in a turbulent environment, *Annu. Rev. Fluid Mech.*, *45*, 293–324, doi: 10.1146/annurev-fluid-011212-140750.
Gunn, R., and G. D. Kinzer (1949), The terminal velocity of fall for water droplets in stagnant air, *J. Meteorol.*, *6*, 243–248.
Heus, T., and A. Seifert (2013), Automated tracking of shallow cumulus clouds in large domain, long duration large eddy simulations, *Geosci. Model Dev.*, *6*(4), 1261–1273.
Heus, T., H. J. J. Jonker, H. E. A. V. den Akker, E. J. Griffith, M. Koutek, and F. H. Post (2009), A statistical approach to the life cycle analysis of cumulus clouds selected in a virtual reality environment, *J. Geophys. Res.*, *114*, D06208, doi:10.1029/2008JD010917.
Jensen, J. B., S. Lee, P. B. Krummel, J. Katzfey, and D. Gogoasa (2000), Precipitation in marine cumulus and stratocumulus. Part I: Thermodynamic and dynamic observations of closed cell circulations and cumulus bands, *Atmos. Res.*, *54*(2), 117–155.
Knight, C. A. (1990), Lagrangian modelling of the ice process: A first-echo case, *J. Appl. Meteorol.*, *29*(5), 418–428.
Kogan, Y. L. (2006), Large-eddy simulation of air parcels in stratocumulus clouds: Time scales and spatial variability, *J. Atmos. Sci.*, *63*, 952–967.
Kostinski, A. B., and R. A. Shaw (2005), Fluctuations and luck in droplet growth by coalescence, *Bull. Am. Meteorol. Soc.*, *86*, 235–244.
Langmuir, I. (1948), The production of rain by a chain reaction in cumulus clouds at temperatures above freezing, *J. Meteorol.*, *5*(5), 175–192.
Lasher-Trapp, S., W. A. Cooper, and A. M. Blyth (2005), Broadening of droplet size distribution from entrainment and mixing in a cumulus cloud, *Q. J. R. Meteorol. Soc.*, *131*, 195–220, doi:10.1256/qj.03.199.
Magaritz, L., M. Pinsky, O. Krasnov, and A. Khain (2009), Investigation of droplet size distributions and drizzle formation using a new trajectory ensemble model. Part II: Lucky parcels, *J. Atmos. Sci.*, *66*, 781–805.
Magaritz-Ronen, L., M. Pinsky, and A. Khain (2014), Effects of turbulent mixing on the structure and macroscopic properties of stratocumulus clouds demonstrated by a Lagrangian trajectory model, *J. Atmos. Sci.*, *71*(5), 1843–1862.
Magaritz-Ronen, L., M. Pinsky, and A. Khain (2016), Drizzle formation in stratocumulus clouds: Effects of turbulent mixing, *Atmos. Chem. Phys.*, *16*, 1849–1862, doi:10.5194/acp-16-1849-2016.
Matheou, G., D. Chung, L. Nuijens, B. Stevens, and J. Teixeira (2011), On the fidelity of large-eddy simulation of shallow precipitating cumulus convection, *Mon. Weather Rev.*, *139*(9), 2918–2939.
Naumann, A. K., and A. Seifert (2015), A Lagrangian drop model to study warm rain microphysical processes in shallow cumulus, *J. Adv. Model. Earth Syst.*, *7*, 1136–1154, doi:10.1002/2015MS000456.
Naumann, A. K., and A. Seifert (2016), Evolution of the shape of the raindrop size distribution in simulated shallow cumulus, *J. Atmos. Sci.*, doi:10.1175/JAS-D-15-0263.1, in press.
Pincus, R., and S. A. Klein (2000), Unresolved spatial variability and microphysical process rates in large-scale models, *J. Geophys. Res.*, *105*, 27,059–27,065.
Pinsky, M., L. Magaritz, A. Khain, O. Krasnov, and A. Sterkin (2008), Investigation of droplet size distributions and drizzle formation using a new trajectory ensemble model. Part I: Model description and first results in a nonmixing limit, *J. Atmos. Sci.*, *65*, 2046–2086.
Rauber, R. M., et al. (2007), Rain in shallow cumulus over the ocean—The RICO campaign, *Bull. Am. Meteorol. Soc.*, *88*, 1912–1924, doi: 10.1175/BAMS-88-12-1912.
Riechelmann, T., Y. Noh, and S. Raasch (2012), A new method for large-eddy simulations of clouds with Lagrangian droplets including the effects of turbulent collision, *New J. Phys.*, *14*, pp. 1–27, doi:10.1088/1367-2630/14/6/065008.
Rogers, R. R., and M. K. Yau (1989), *A Short Course in Cloud Physics, Int. Ser. Nat. Philos., vol. 113*, 3rd ed., Elsevier, Oxford, U. K.
Seifert, A. (2008), On the parameterization of evaporation of raindrops as simulated by a one-dimensional rainshaft model, *J. Atmos. Sci.*, *65*, 3608–3619.
Seifert, A., and K. D. Beheng (2001), A double-moment parameterization for simulating autoconversion, accretion and selfcollection, *Atmos. Res.*, *59-60*, 265–281.
Seifert, A., and T. Heus (2013), Large-eddy simulation of organized precipitating trade wind cumulus clouds, *Atmos. Chem. Phys.*, *13*(1), 5631–5645, doi:10.5194/acp-13-5631-2013.
Seifert, A., and B. Stevens (2010), Microphysical scaling relations in a kinematic model of isolated shallow cumulus clouds, *J. Atmos. Sci.*, *67*(5), 1575–1590.
Shaw, R. A. (2003), Particle-turbulence interactions in atmospheric clouds, *Annu. Rev. Fluid Mech.*, *35*, 183–227.
Shima, S., K. Kusano, A. Kawano, T. Sugiyama, and S. Kawahara (2009), The super-droplet method for the numerical simulation of clouds and precipitation: A particle-based and probabilistic microphysics model coupled with a non-hydrostatic model, *Q. J. R. Meteorol. Soc.*, *135*, 1307–1320, doi:10.1002/qj.441.
Simpson, G. C. (1941), On the formation of cloud and rain, *Q. J. R. Meteorol. Soc.*, *67*(290), 99–133.
Stevens, B. (2007), On the growth of layers of non-precipitating cumulus convection, *J. Atmos. Sci.*, *64*, 2916–2931.
Stevens, B., and A. Seifert (2008), Understanding macrophysical outcomes of microphysical choices in simulations of shallow cumulus convection, *J. Meteorol. Soc. Jpn.*, *86*, 143–162.
Stevens, B., G. Feingold, W. R. Cotton, and R. L. Walko (1996), Elements of microphysical structure of numerically simulated nonprecipitating stratocumulus, *J. Atmos. Sci.*, *53*(7), 980–1006.
Stevens, B., et al. (2005), Evaluation of large-eddy simulations via observations of nocturnal marine stratocumulus, *Mon. Weather Rev.*, *133*, 1443–1462.
Sui, C.-H., X. Li, and M.-J. Yang (2007), On the definition of precipitation efficiency, *J. Atmos. Sci.*, *64*(12), 4506–4513.
Telford, J. (1955), A new aspect of coalescence theory, *J. Meteorol.*, *12*(5), 436–444.
Vaillancourt, P., and M. Yau (2000), Review of particle-turbulence interactions and consequences for cloud physics, *Bull. Am. Meteorol. Soc.*, *81*, 285–298.
van Zanten, M. C., et al. (2011), Controls on precipitation and cloudiness in simulations of trade-wind cumulus as observed during RICO, *J. Adv. Model. Earth Syst.*, *3*, M06001, doi:10.1029/2011MS000056.
Yang, F., M. Ovchinnikov, and R. A. Shaw (2015), Long-lifetime ice particles in mixed-phase stratiform clouds: Quasi-steady and recycled growth, *J. Geophys. Res. Atmos.*, *120*, 11,617–11,635, doi:10.1002/2015JD023679.